

Trond Erik Havre

Near-IR spectroscopy as a method for studying the formation of calcium naphthenate

Received: 6 December 2002
Accepted: 28 April 2003
Published online: 3 September 2003
© Springer-Verlag 2003

T.E. Havre
Ugelstad Laboratory,
Department of Chemical Engineering,
Norwegian University of Sciences
and Technology, 7491 Trondheim,
Norway
E-mail: trond.havre@champion-servo.com

Abstract A method for studying the precipitation of calcium naphthenate particles by means of near-IR spectroscopy is presented. Naphthenic or fatty acids were dissolved in water at high pH (11.2–11.5). Upon addition of a Ca^{2+} solution the nucleation period and particle growth were monitored. The near-IR spectra experience a baseline elevation owing to the formation and growth of calcium naphthenate particles. The resulting change in optical density over time is discussed on the basis of supersaturation, particle sizes, agglomeration, Ca^{2+} -to-carboxylic acid ratio and nucleation

process. Solubility products, defined as the ion concentration products where no particle growth was detected, were estimated for the calcium soaps. The method showed some quantitative limitations since the particle sizes changed with supersaturation. Smaller particles will have less influence on the optical density and the larger particle will dominate the resulting scattering contribution. However, it is obvious that the method has qualitative value, for example, to study the efficiency of different calcium naphthenate inhibitors.

Introduction

In recent years there has been an increase in the production of acidic crude oils with high amounts of naphthenic acids [1, 2]. Naphthenic acids are classified as monobasic carboxylic acids with the general formula RCOOH , where R represents a cycloaliphatic structure. The term “naphthenic acid” is generally used to account for all carboxylic acids present in crude oil, including acyclic and aromatic acids [3]. These naphthenic acids show polydispersity in size and structure [4, 5, 6, 7, 8, 9, 10]. The smallest molecules are readily dissolved in the aqueous phase at pH 5, while the larger molecules are preferably oil-soluble. Most of these homologs dissolve in an aqueous phase at elevated pH [11, 12, 13].

Under certain conditions the naphthenic acids will precipitate with Ca^{2+} ions present in the water produced and form calcium naphthenate. This precipitation accumulates predominantly in oil/water separators and

desalters, but naphthenates can also deposit in the tubes and pipelines [1, 2, 14, 15, 16].

In order to avoid formation of naphthenate deposit in crude oil producing equipment, a better understanding of the formation mechanism is needed. In this study it is shown that near-IR (NIR) spectroscopy is applicable as a tool to study the formation and growth of calcium naphthenate particles.

Several authors have reported the use of NIR spectroscopy for the determination of particle sizes, often in combination with multivariable analysis [17, 18, 19, 20]. In a previous paper we used NIR spectroscopy to follow the disintegration of asphaltene particles by various amphiphiles in a heptane/toluene model system [21]. The main advantage of the NIR spectroscopy technique is that it can be performed online. In addition, it has the advantages of speed, simplicity, low-operating cost and the possibility to correlate several properties to one single spectrum. Optical fibers can be used to carry the

light from the light source to the point of measurement and back to the light detector. This makes NIR spectroscopy applicable in many industrial processes, for example, in high-pressure environments [22].

Theory

Crystallization

The theory behind crystallization was described in detail by Mullin [23]. The first step in a crystallization process is nucleation. While secondary crystallization is induced by crystals already present, primary nucleation occurs either spontaneously (homogeneous) or is induced by foreign particles (heterogeneous).

Induction period

A period of time elapses between the achievement of supersaturation and the appearance of crystals. This time lag, generally referred to as an “induction period”, is influenced by the supersaturation, the state of agitation, the presence of impurities, viscosity, etc. The induction period, t_{ind} , can be considered as being made up of several parts defined by Eq. (1).

$$t_{\text{ind}} = t_r + t_n + t_g, \quad (1)$$

where t_r is the “relaxation time” required for the system to achieve a quasi-steady-state distribution of molecular clusters, t_n is the time necessary to form a stable nucleus and t_g is the time needed for the particle to grow to a detectable size. The nucleation time depends mainly on temperature, supersaturation and the interfacial tension between the solution and the solid formed.

The rate of nucleation, J , i.e. the number of nuclei formed per unit time per unit volume, can be expressed as

$$J = A \exp\left(\frac{16\pi r \gamma^3 v^2}{3k^3 T^3 (\ln S)^2}\right), \quad (2)$$

where A is a constant, r is the particle radius, γ is the interfacial tension, v is the molecular volume, k is the Boltzmann constant, T is the temperature and S is the supersaturation. For systems involving sparingly soluble salts, S can be defined as the ratio of the ion concentration product, Q , to the solubility product, K_{sp} . For a calcium naphthenate system this will be according to Eq. (3):

$$S = \frac{[\text{Ca}^{2+}] \cdot [A^-]^2}{[\text{Ca}^{2+}]_{\text{eq}} \cdot [A^-]_{\text{eq}}^2} = \frac{Q}{K_{\text{sp}}}, \quad (3)$$

where $[\text{Ca}^{2+}]$ and $[A^-]$ are the actual concentration of calcium ions and dissociated acid respectively. $[\text{Ca}^{2+}]_{\text{eq}}$

and $[A^-]_{\text{eq}}$ are the concentrations in an aqueous solution in equilibrium with the solid salt.

The induction period cannot be regarded as a fundamental property since it is affected by many external influences. However, by making the assumption that it is inversely proportional to J it can give information about the nucleation process. The induction period will then depend on the supersaturation according to Eq. (4):

$$\log t_{\text{ind}} \propto \frac{\gamma^3}{T^3 (\log S)^2}. \quad (4)$$

Hence, a plot of $\log t_{\text{ind}}$ versus $(\log S)^{-2}$ will give a straight line with a slope dependent on the temperature and the interfacial tension.

Growth period

The induction period is followed by a period where the particles grow. In order to understand the kinetics of this process, several different mechanisms are proposed. The surface-energy theories claim that the shape the growing crystals assume is that which has a minimum surface area. The diffusion theories presume that matter is deposited at the surface owing to the concentration gradient between the bulk solution and at the surface. Adsorption layer theories assume that the crystals grow by a layer-by-layer adsorption process.

Burton, Cabrera and Frank have proposed a relationship between the growth rate and the supersaturation, i.e. the BCF relationship, given by Eq. (5) [23]:

$$R = A(S-1)^2 \tanh\left(\frac{B}{S-1}\right), \quad (5)$$

where R is the rate of crystallization, S is the supersaturation and A and B are complex temperature-dependent constants. At low supersaturations the rate of reaction is proportional to $(S-1)^2$, while at high supersaturations it is proportional to $(S-1)$. Other models end up with a similar result. Owing to the complexity of the crystallization processes empirical models, as given in Eq. (6), are readily used [24]:

$$R = k(S-1)^n, \quad (6)$$

where k is a constant and n is the effective order of crystallization.

Other factors that will influence the growth rate are the particle size, agitation, the ratio of positive to negative reacting ions, the temperature, etc. Experiments performed by Chivate et al. [25] showed that the growth rate of barium soap particles had higher values at low temperature than at high temperature, whereas the nucleation rates had lower values at lower temperatures.

Light scattering by particles

When light is sent through a chemical sample not all the light is transmitted. This can be accounted for by two distinct mechanisms: electronic absorption by the different molecules and scattering from particles or aggregates. Owing to the light scattering, the NIR spectra will display a baseline elevation that is dependent on the size of the particles. Hence, by monitoring the baseline elevation, the growth of particles can be followed. Light scattering in the NIR region is described in detail by Mullins [26] and Kenker [27]; a brief description is given in the following.

The light scattering can be divided into two groups: wavelength-independent scattering, where the size of the particles is large compared to the wavelength of the light, and wavelength-dependent scattering, where the particles are of comparable size to or smaller than the wavelength of the light. The latter group contains the case of $r/\lambda \leq 0.05$, where λ is the wavelength of light and r the particle radius. At this so-called Rayleigh condition, the particle is so small that the electromagnetic field it experiences is uniform over the particle. By also assuming that the particles are slightly lossy and dielectric, an expression for the scattering cross-section of a particle is given by Eq. (7):

$$\sigma_{sc} = \frac{2^7 \pi^5}{3} \frac{r^6}{\lambda^4} \left(\frac{n^2 - 1}{n^2 + 2} \right)^2, \quad (7)$$

where r is the particle radius, λ is the wavelength of the incident light and n is the ratio of the discrete phase to the continuous phase index of refraction. In the absence of multiple scattering, and in the Rayleigh limit ($r/\lambda \leq 0.05$), fewer, but larger, spheres are much more efficient scatterers than the same mass of smaller particles.

Within the Rayleigh limit the light extinction can be considered to be the sum of the absorbance and scattering contributions, represented by the particle cross-sections:

$$\sigma_{tot} = \sigma_{sc} + \sigma_{abs}, \quad (8)$$

where σ_{tot} , σ_{sc} and σ_{abs} are the total, the scattering and the absorption cross-sections, respectively. The absorption cross-section scales with r^3 , while the scattering cross section scales with r^6 ; hence, the change in the total cross-section as a result of particle growth is governed by the scattering contribution.

By utilizing a wavelength of 1,280 nm the Rayleigh condition is only satisfied for particles with radius up to 64 nm. Heller [28] investigated the error introduced when the particle sizes are beyond that of the Rayleigh regime. The error was found to be less than 5% for $r/\lambda \leq 0.25$. For $\lambda = 1,280$ nm this corresponds to a particle size of 320 nm. For even larger particles the optical

density (OD) will still relate to the radius but with a power less than 6.

The OD is given by [26]

$$OD = \log \left(\frac{I_0}{I} \right) = 0.434 N \sigma_{tot}, \quad (9)$$

where I and I_0 are the intensities of the transmitted and incident light, respectively, and N is the number of particles in the total cross-section σ_{tot} .

The measured OD is thus a combination of absorption and scattering contributions. The effect of multiple scattering is not accounted for in this equation. Absence of multiple scattering implies that radiation scattered by a single particle proceeds directly to the detector without any further scattering encounters. In the case of multiple scattering, the scattering and absorption cannot be treated separately. Conditions for single scattering can usually be attained by working with dilute systems and with small volumes.

Experimental

Chemicals

All the chemicals were used as supplied. $\text{CaCl}_2 \cdot 2\text{H}_2\text{O}$ (p.a.) and NaOH (p.a.) were supplied by Merck. Information for the carboxylic acids used is given in Table 1. The naphthenic acid from a crude oil fraction was extracted with an ion-exchange method as described by Mediaas et al. [29].

Methods

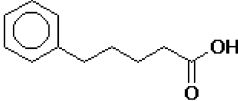
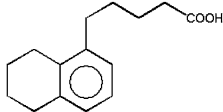
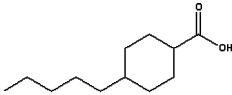
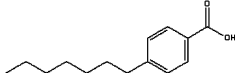
The NIR measurements were performed with a Brimrose AOTF Luminar 2000 spectrometer equipped with a fiber optic sampling probe for transmittance measurements. The wavelength region was set to 1,100–2,200 nm, the total number of scans per spectrum to 32 and the total path length was 1 mm.

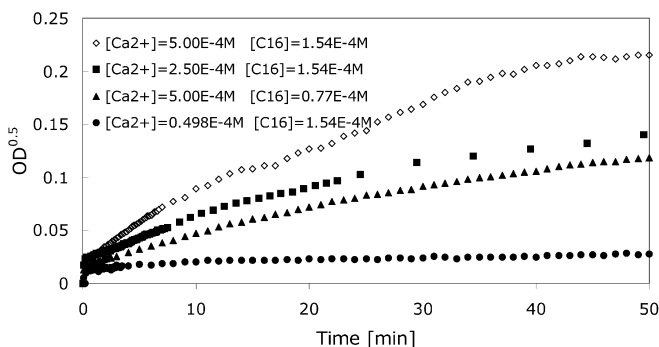
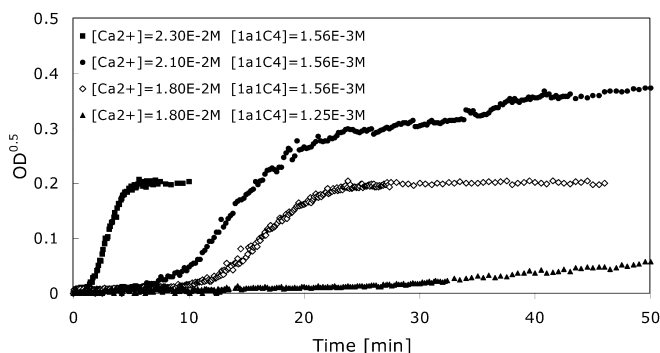
In each experiment, one of the five carboxylic acids listed in Table 1 was dissolved in NaOH with pH 11.5. The addition of carboxylic acid led to a decrease in pH; however, if full dissociation is assumed, the pH cannot fall below 11.2 for any of the experiments in this study. The pH was chosen to be high enough for the carboxylic acid to be soluble in the water phase and low enough to hinder the formation of $\text{Ca}(\text{OH})_2$ upon addition of Ca^{2+} . To hasten the process of dissolving the acid, the solution was heated to 70 °C. The experiments were performed at room temperature (22 °C) and under a nitrogen atmosphere to avoid formation of CaCO_3 . The solution was stirred under a nitrogen atmosphere for about 10 min before the Ca^{2+} solution was added. In the study of particle growth, the absorbance at 1,280 nm was utilized. The reason for this choice is that the absorption from the aqueous phase is minimal in this region, and that this is the NIR region with the least noise in the measurements.

Results and discussion

Carboxylic acids and Ca^{2+} were mixed at different concentrations at high pH and the particle growth was

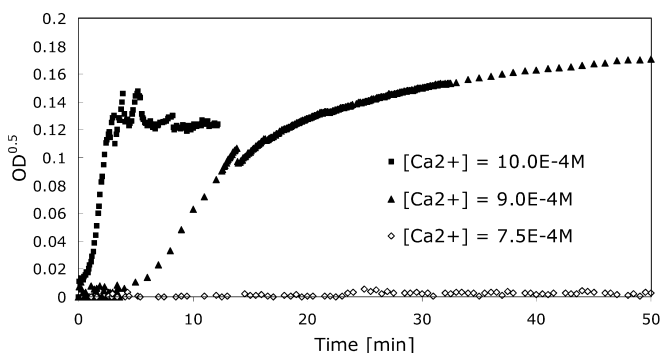
Table 1 Carboxylic acids

Name	MW [g/mol]	Chemical structure	Source	Purity [wt%]
[a1C4] 5-phenylpentanoic acid	172		University of Bergen	> 99
[1a1C4] 1-Naphtalene-pentanoic acid, 5,6,7,8-tetrahydro-	232		University of Bergen	> 99
[C51] trans-4-n-Pentylcyclohexanecarboxylic acid	198		TCI	> 99
[C7a1] 4-heptylbenzoic acid	220		Acros Organics	> 99
[C16] n-hexadecanoic acid	256	CH ₃ (CH ₂) ₁₄ COOH	Fluka	> 99
Naphtenic acid extracted from crude oil fraction	~320	mixture		> 90

**Fig. 1** Square root of the optical density (OD) at 1,280 nm versus time for different concentration of Ca^{2+} and hexadecanoic acid ($C16$)**Fig. 2** $OD^{0.5}$ at 1,280 nm versus time for different concentration of Ca^{2+} and 1a1C4

monitored with NIR spectroscopy. The addition of Ca^{2+} started at time zero and Ca^{2+} was added dropwise over a period of 10–20 s. The square root of the OD at 1,280 nm is shown in Figs. 1, 2, 3 and 4 versus time for experiments with carboxylic acids, labeled C16, 1a1C4, C51 and C7a1, respectively. The structures of the carboxylic acids are given in Table 1.

The reason for plotting the square root of the OD is that the OD depends on the sixth power of the radii or the square of the volume of the particles. Hence, a change in the square root of the OD can serve as a measurement of the change in the total amount of precipitate. The square root of the OD is directly proportional to the particle volume in systems consisting of a constant number of monodisperse particles. In the

**Fig. 3** $OD^{0.5}$ at 1,280 nm versus time for different concentrations of Ca^{2+} and C51. The concentration of C51 is 1.56×10^{-3} M

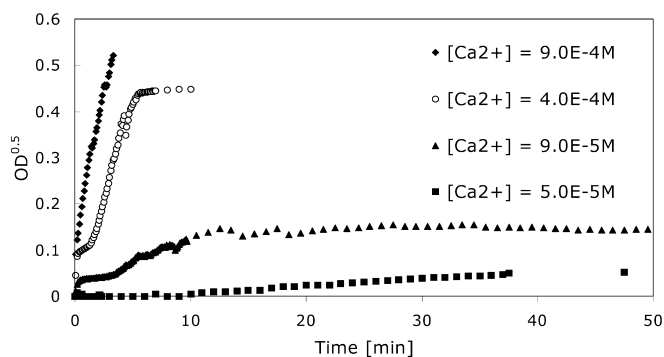


Fig. 4 $OD^{0.5}$ at 1,280 nm versus time for different concentrations of Ca^{2+} and C7a1. The concentration of C7a1 is 1.56×10^{-3} M

systems investigated, with polydisperse particles, the larger particles will govern the resulting OD since they contribute much more to the OD than the small particles. The number of particles is also unknown. Nevertheless, the curves give a good qualitative description of the calcium naphthenate formation.

Induction period

The induction period is the period where nucleation and growth of the nucleus to a detectable size occurs. This period is seen for some of the experiments with 1a1C4, C51 and C7a1 (Figs. 2, 3, 4). The induction period for all the experiments with C16 is too short to be detected (Fig. 1). The induction period can be set up as the sum of different contributions according to Eq. (1). The relaxation time, t_r , is believed to be of the order of $10^{-17}D$, where D is the diffusivity (meters squared per second) [23]. This means that in a water solution with $D \sim 10^{-9} \text{ m}^2 \text{ s}^{-1}$, the relaxation time would be around 10^{-8} s. The contribution from this term will hence be of little importance in the systems investigated here. For systems with high viscosity, the diffusivity will be considerably higher, resulting in a significant relaxation period. The next term, t_n , is the time necessary to obtain a stable nucleus. This term is shown to depend on the supersaturation; however, its estimation is the subject of speculation. The time for growth to detectable particles, t_g , obviously depends on how small particles the instrumentation is able to detect. With NIR spectroscopy it was shown by Aske et al. [30] that particles can be detected when they reach a size of about $r = 30$ nm. The mechanism and kinetics of growth of a nucleolus are believed to be different than for macrocrystals. This quantity is therefore also difficult to predict.

By making the assumption that the induction period is inversely proportional to the rate of nucleation, it can give information about the nucleation process. The induction period will then depend on the supersaturation according to Eq. (4).

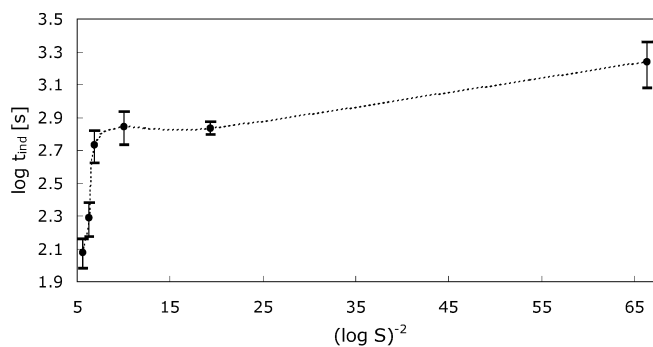


Fig. 5 The logarithm of the induction period as a function of $(\log S)^{-2}$ for 1a1C4

The logarithm of the induction period for systems consisting of 1a1C4 is plotted in Fig. 5 versus $(\log S)^{-2}$. The error bars illustrate the uncertainty in reading the induction periods from the $OD^{0.5}$ versus time curves. The lower error bar represent the time where an increase in the OD is detected, while the upper error bars represent the times where the growth rate becomes constant. The points are average values of these two times. It is seen that the trend of the curve in Fig. 5 is less affected by how the induction period is recorded. For ideal homogeneous nucleation, the plot would give a straight line according to Eq. (4). At high supersaturations (to the left in the figure) $\log t_{\text{ind}}$ depends linearly on $(\log S)^{-2}$. A sudden decrease in the slope of the curve is then seen when approaching lower levels of supersaturation. This indicates a change in the interfacial tension between the solid and the water. Two factors can explain this behavior. The change in the curve at $(\log S)^{-2} \sim 10$ can be due to a transition from heterogeneous to homogeneous nucleation. At high supersaturation, the nucleation is homogeneous and at lower supersaturation the nucleation becomes heterogeneous. The reason for this is that the concentration of impurities, leading to heterogeneous nucleation, will be constant in the system independent of the supersaturation. Since the rate of homogeneous nucleation is lower for lower supersaturations, the heterogeneous nucleation process will dominate. Another explanation is that the change in slope is due to the agitation. Mullin and Zacek [31] have shown that the slope of the $\log t_{\text{ind}}$ versus $(\log S)^{-2}$ curve decreases at higher values of $(\log S)^{-2}$ for agitated systems. However, the change in the slope of their curves was continuous, so the agitation effect cannot explain the shape of the curves in Fig. 5 alone. A transition from heterogeneous to homogeneous nucleation is hence likely.

A detailed description of the induction period for C51 (Fig. 3) is not possible with the amount of data collected for this system. However, by studying Fig. 3 it is evident that increased supersaturation leads to a decrease in the induction period. The same is seen for C7a1 in Fig. 4.

The experiment with the lowest supersaturation of C7a1 gives an induction period as expected. For the experiment with moderate supersaturations there is a sudden increase in $OD^{0.5}$ upon addition of Ca^{2+} solution, followed by a period with little increase in $OD^{0.5}$ which can be confused with an induction period. The sudden increase corresponds most probably to the rapid formation of a nucleus and an induction period that is too short to be detected. The initial low $dOD^{0.5}/dt$ is discussed in the next section.

The NIR spectroscopy technique presented here can measure induction periods when they last for a certain time. When the induction period is less than about 5 s, difficulties arise. The mixing time of the solutions with the reactants can in this case be comparable with or exceed the measured induction period. In the experiments performed here, 10–20 s was allowed for the addition of calcium to the solution with carboxylic acid. In this case, if the induction period is determined to a value under 30 s, the uncertainty will be large. If the Ca^{2+} solution is added too fast, there is a chance that high local concentration of Ca^{2+} can initiate the precipitation.

Growth period

For all the systems investigated, higher concentration of acid and calcium ions led to an increase in the slope of the OD versus time curves after the induction period, representing an increase in the rate of reaction.

The slope of $OD^{0.5}$ versus time, representing the rate of crystallization, is plotted in Fig. 6 as a function of $(S-1)^2$ for 1a1C4. A linear relationship is seen for the lower supersaturations, which is in accordance with the BCF relationship (Eq. 5). The slope of the curve increases for higher supersaturations. According to the model, the rate of reaction at higher supersaturation would approach proportionality to $(S-1)$. Instead $dOD^{0.5}/dt$ becomes more dependent on the supersaturation. The increase in the slope occurs at the same

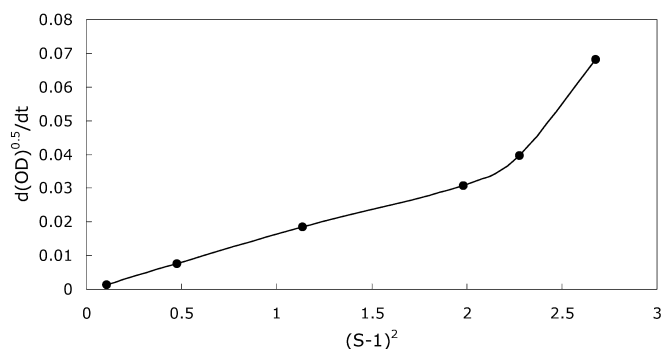


Fig. 6 $d(OD^{0.5})/dt$ versus $(S-1)^2$ for 1a1C4

supersaturation level ($S \sim 1.4$) as where the dependence of $\log t_{ind}$ versus $(\log S)^{-2}$ changes in Fig. 5. It was suggested that a transition from heterogeneous to homogeneous nucleation occurred at $S \sim 1.4$. If the nucleation process is heterogeneous the number of nuclei will be considerably lower than if homogeneous nucleation occurs. The sizes of the particles are more important than the number for the response of the OD. For a given value of $dOD^{0.5}/dt$, the actual crystallization rate will be higher for systems with a large number of small particles than for a system consisting of a lower number of large particles. It is therefore expected that when going from a system where heterogeneous nucleation occurs, and the number of particles is low, to a system with a large number of particles, the dependency of $dOD^{0.5}/dt$ on $(S-1)$ would decrease. Instead, the dependency increases. The behavior may be explained as a result of agglomeration. The rate of agglomeration will obviously depend on the number of particles. Hence, the increase in the slope of the curve in Fig. 6 can be due to increased agglomeration as the number of particles increases, which in turn is a result of homogeneous rather than heterogeneous nucleation. When particles agglomerate, the OD will increase even though the volume of the precipitated material remains constant. Ostwald ripening may also be of importance. Ostwald ripening is the process in which small particles dissolve and the solute subsequently deposits on the larger particles. The driving force of this process is the lowering of the total surface energy. An additional explanation is that the total area becomes larger for small particles. It is expected that this will increase the rate of crystallization. The results may be influenced by the fact that for a distribution of particle sizes, the largest particles will govern the resulting OD.

Evidence for the formation of smaller particles at high supersaturation can be found by studying Fig. 2. The curve with the highest supersaturation (to the left) reaches a final OD lower than expected. The final value increases with supersaturation for the other experiments. This indicates that even if the experiment with the highest supersaturation yields the highest amount of solid material, the particles are small and therefore their scattering efficiency is bad. It has been argued that agglomeration occurred in the 1a1C4 systems with high supersaturation. If agglomeration occurs, the rate of agglomeration is not sufficient to create particles that are of the same size as for less supersaturated systems. Increased aggregation can still explain the trend in Fig. 6.

The rate of crystallization for the other acids shows a different dependence on the supersaturation. The empirical relation, given in Eq. (6), was used for this evaluation. The slope of $OD^{0.5}$ versus time is proportional to $(S-1)^n$, where n is 0.4 and 0.5 for C16 and C7a1, respectively. For C51 the best fit was found to be for $n=0.2$, but this was based on only three points,

making the uncertainty large. The dependency of the supersaturation on the crystal growth followed the same trend for all the different levels of supersaturation investigated for each of these three acids. Several different mechanisms will influence how $dOD^{0.5}/dt$ relates to the supersaturation. A transition from heterogeneous to homogeneous nucleation may occur at higher supersaturation. Independently of whether this happens the number of particles is expected to be higher for higher levels of supersaturations. The reason for this is that supersaturation affects the nucleation rate more than the growth rate [32]. Therefore, at high supersaturations the number of particles increases more than the size, giving rise to a smaller effect on the increase in the OD. On the other hand, an increased number of particles can lead to increased aggregation, which will have a positive effect on $dOD^{0.5}/dt$. The particles tendency to agglomerate upon collision is therefore of importance. For the particles to be stable against agglomeration, the ratio of acid to calcium may be of importance. Precipitation phenomena of calcium oleate in aqueous solution have been studied by Matijević et al. [33]. It was shown that a ratio of oleate ions to Ca^{2+} of 2:1 gave solutions with the highest turbidity. Excess of either of the two ions led to the formation of small particles that were stable to coalescence owing to electrostatic stabilization. Small particles will contribute less to the turbidity as discussed earlier. Precipitation phenomena of colloidal laurate soap particles with different cations were studied by Young et al. [34]. They came to the same conclusion regarding particles of calcium and copper laurate. For thallium and lanthanum laurate the systems were influenced by the formation of complex ions. With this background, It is likely that agglomeration of particles will be most prominent in systems where the ratio of Ca^{2+} to dissociated acid is 1:2. However, a high electrolyte concentration in the water will decrease the ability of the particles to be stabilized electrostatically towards agglomeration. For the C51 systems the ratios between Ca^{2+} and acid were close to 1:2 (1.3:2.0, 1.2:2.0, 1:2.1). In this case the tendency to agglomerate upon collision is expected to be high. However, $dOD^{0.5}/dt$ depends on $(S-1)$ with an exponent equal to 0.2, indicating that the agglomeration rate is low. A high rate of agglomeration would result in a higher value of the exponent. The lack of charge surfaces is hence not enough for the particles to agglomerate in this case.

In the experiments with the other carboxylic acids, one of the reactants was in most cases in excess. In experiments with 1a1C4 the ratio of Ca^{2+} to acid was in the range 23:2–30:2. The excess of Ca^{2+} could be expected to stabilize the particles formed. Nevertheless, agglomeration was suggested to occur in these systems. It is evident that even if the ratio between the reactants most probably influence the agglomeration stability of the particles, it cannot explain the different results ob-

tained regarding the dependency of $dOD^{0.5}/dt$ on $(S-1)$. The low $dOD^{0.5}/dt$ at high supersaturation is most probably the result of the formation of small particles. As stated earlier, small particles will contribute less to the OD.

The growth period of the C7a1 systems with moderate supersaturation differs from the other acids studied in that $dOD^{0.5}/dt$ has a low value right after the induction period (Fig. 4). It is seen that the induction period is very short, indicating a fast rate of nucleation, which in turn will lead to a large number of nuclei. When the number of particles is large, the response in $OD^{0.5}$ will be weak. The reason for the later increase in the slope of $OD^{0.5}$ versus time must be due to a reduction in the number of particles. This can occur by agglomeration and/or Ostwald ripening. A large number of particles will facilitate a high rate of agglomeration.

All the carboxylic acids were added to water solution with pH 11.5. Since the concentration of acid was different in some experiments, a different pH in the water phase is expected. However, even if all the acid were dissociated, the pH would not fall below 11.2 in any experiment. Matijević et al. [33] claimed that pH fluctuation between 9 and 11.5 did not influence the precipitation of calcium oleate. It is therefore not expected that the fluctuation of the pH between 11.2 and 11.5 will influence the results presented here. The presence of micelles can influence the crystallization process. The critical micelle concentration (cmc) for all the carboxylic acids used in this study, except C41a1, has been reported by Havre and Sjöblom [35]. The cmc values are too high for micelles to influence the systems reported here. The formation of micelles may be of influence in 1a1C4-systems if the cmc is below $1.6 \times 10^{-3} \text{ mol dm}^{-3}$.

Steady-state period

After the induction and growth period the OD reaches a constant value in most experiments. The reason for this is most likely that the concentration of acids and Ca^{2+} in the solution is near the values corresponding to the solubility product, so there is equilibrium between solid calcium carboxylate and ions. The particles can still grow by agglomeration and Ostwald ripening. The ability of the particles to scatter light will increase with their size only up to a certain size. Hence, the particles will not contribute to an increase in the OD when the particles become large, and their growth will not be detected by monitoring the OD. Because the number of small particles decreases, a decrease in the OD may be seen. In some cases a sudden increase in the OD sets in. If the agitation is increased, the OD falls again, indicating that the increase was due to larger particles that had attached to the NIR spectroscopy probe.

Estimation of solubility products

As the amount of Ca^{2+} and carboxylic acid is decreased, the response in the NIR spectroscopy measurements will eventually become zero. The concentration at which this happens can be used to estimate the solubility products, K_{sp} , for the different calcium soaps. The solubility products were found by extrapolating a curve of $\text{dOD}^{0.5}/\text{dt}$ versus the ion concentration product to $\text{dOD}^{0.5}/\text{dt}=0$. The K_{sp} values are given in Table 2. The solubility products are plotted versus the molecular weight of the acidic form in Fig. 7.

It is shown that for four of the acids the logarithm of the solubility product is linearly dependent on the molecular weight of the acids. However, 1a1C4 does not follow the same trend, having a considerably higher K_{sp} than expected from its molecular weight. The presence

Table 2 Solubility products for the calcium salt of different carboxylic acids. (Detailed information on the acids is given in Table 1)

Shortname	Chemical structure	K_{sp} [$\text{mol}^3 \text{dm}^{-3}$]
[a1C4]		6.1E-8
[1a1C4]		2.8E-8
[C51]		2.2E-9
[C7a1]		1.2E-10
[C16]	$\text{CH}_3(\text{CH}_2)_{14}\text{COOH}$	6.4E-13

Fig. 8 $\text{OD}^{0.5}$ at 1280 nm versus time for experiments with two different stirring speeds ($[\text{C16}] = 7.7 \times 10^{-5} \text{ M}$ and $[\text{Ca}^{2+}] = 5.0 \times 10^{-4}$). Triangles represent lower stirring speed

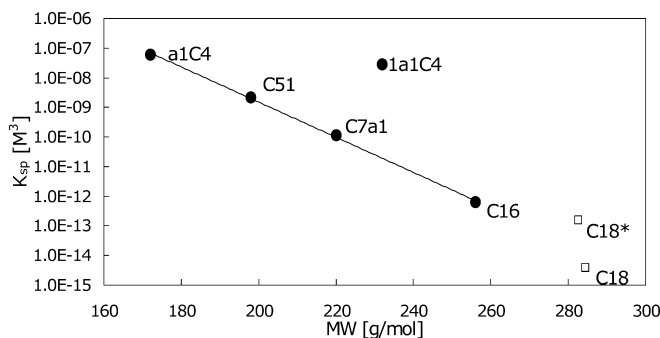
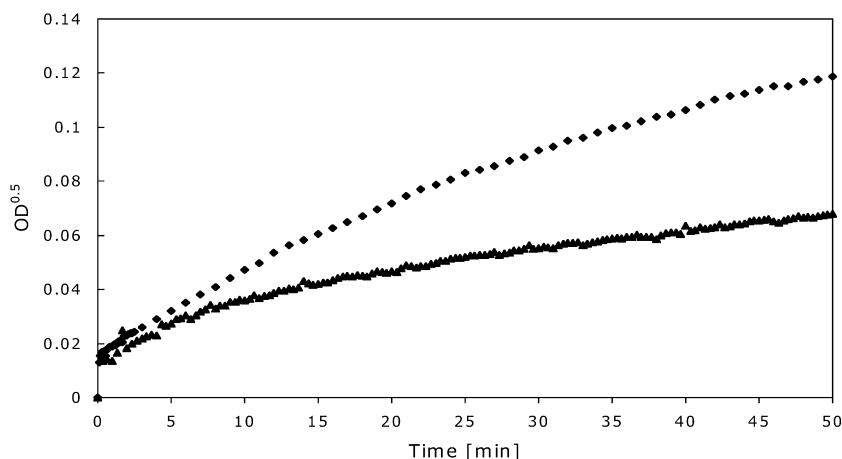


Fig. 7 Solubility products for different carboxylic acids. The values for calcium stearate (C18) and calcium oleate (C18*) are from Ref. [36]. The other abbreviations are explained in Table 1

of the aromatic ring structure will make the molecule hydrophilic. Two of the other molecules also contain an aromatic ring, so the K_{sp} value is still unexpectedly high. If the acid molecules are able to form some sort of complexes in water, this will make the predicted solubility constant too high. K_{sp} values for calcium stearate, C18, and calcium oleate, C18*, determined by surface tension measurements have been reported by Beneventi et al. [36]. These values are plotted in Fig. 7 for comparison.

The ion concentration product is said to be equal to K_{sp} when no response is seen in the NIR spectroscopy measurements. If small not detectable particles are present at low ion concentration products, this method will give slightly higher K_{sp} values than other methods.

Agitation

Agitation is a crucial parameter in crystallization experiments. The $\text{OD}^{0.5}$ is shown versus time in Figure 8 for two experiments with equal concentration of C16 and Ca^{2+} , but with different stirring speeds. It is seen that the agitation condition influences the system significantly. When performing these experiments it became evident that equal stirring conditions were of great importance in order to get reproducible results. The use

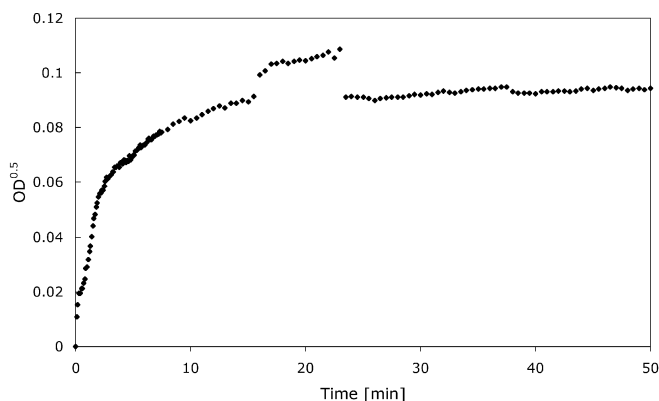


Fig. 9 $OD^{0.5}$ at 1,280 nm versus time for 3.0×10^{-2} M Ca^{2+} and 1.12×10^{-4} M naphthenic acid extracted from a crude oil

of a slightly smaller magnet on the magnet stirrer influenced the results significantly. Increased agitation will lead to an increase in the rate of a diffusion-controlled nucleation process. However, it has been shown by Mullin and Raven [37, 38] that an increase in the intensity of the agitation does not necessarily lead to a continuous enhancement of the nucleation process. They found that in some cases increased agitation led to decreased nucleation. They suggested that the reason for this was that while increased stirring will increase the nucleation rate in a diffusion-controlled process, it will also lead to increased attrition. For agitation to affect the growth of particles, the mechanism for growth must be controlled by diffusion of reactant from the bulk solution to the surface of the growing particles. Although this diffusion can control the rate of crystallization, it has been shown that this mechanism alone is not sufficient to explain the mechanism of crystallization. Agitation will increase the number of collisions between particles and hence increase the rate of agglomeration.

Naphthenic acid from crude oil

One of the reasons for studying the formation of calcium naphthenate is its relevance to the industrial problem of deposition of calcium naphthenate in crude oil producing equipment. Hence, systems with naphthenic acids

from crude oil are of interest. Naphthenic acid was extracted from a crude oil fraction. The mean molecular weight of the resulting naphthenic acid mixture was around 320 g mol^{-1} . An experiment with $1.12 \times 10^{-4} \text{ mol dm}^{-3}$ naphthenic acid and $3.0 \times 10^{-2} \text{ mol dm}^{-3}$ Ca^{2+} was set up and the result of this experiment is given in Fig. 9.

The induction period for this system is short, indicating the sudden formation of a nucleus upon addition of Ca^{2+} . The reason for the higher OD between 15 and 25 min is probably temporary attachment of particles to the NIR spectroscopy probe. The most important result from this experiment is that it is shown that the NIR spectroscopy method can be used in studying a mixture of naturally occurring naphthenic acids. In such a system a detailed theoretical study of the mechanism is not possible. Qualitative results as shown in Fig. 9 can be used, for example, to study the efficiency of different calcium naphthenate inhibitors.

Conclusions

A method for studying the precipitation of calcium naphthenate in the aqueous phase has been presented in this paper. It was shown that the induction period can be determined. To obtain a good result, the induction period ought to be at least over 30 s. Information about the rate of reaction for particle growth can be obtained; however, its quantitative value is uncertain. This is because the number of particles and the total amount of precipitate are not known at a given time. In addition, for a distribution of particles sizes, the larger particles will govern the resulting scattering contribution. The rate of nucleation versus the rate of growth, agglomeration, particles sizes and Ostwald ripening will influence the results. Solubility products can also be estimated. Although the method has some quantitative limitations, it is obvious that it has qualitative value, for example, to study the efficiency of different calcium naphthenate inhibitors.

Acknowledgements T.E.H. acknowledges the technology program FLUCHA II, financed by the Research Council of Norway and the oil industry, for a doctoral grant. Cory Searcy is acknowledged for assistance with the experimental work and Statoil R&D Centre is thanked for offering the use of laboratory facilities.

References

1. Goldszal A, Hurtevent C, Rousseau G (2002) In: SPE oilfield scale symposium, SPE74661 1-11, Aberdeen, UK, 2002
2. Rousseau G, Zhou H, Hurtevent C (2001) In: SPE oilfield scale symposium, SPE68307 1-8, Aberdeen, UK, 2001
3. Brient JA, Wessner PJ, Doyle MN (1995) In: Kirk-Othmer Encyclopedia of chemical technology. Wiley, New York, p 1017-1029
4. Fan, T-P (1991) Energy Fuels 5:371-375
5. Hsu CS, Dechert GJ, Robbins WK, Fukuda EK (2000) Energy Fuels 14:217-223
6. Koike L, Reboucas LMC, Reis FdA, Marsaioli AJ, Richnow HH, Michaelis W (1992) Org Geochem 18:851-860

7. Acevedo S, Escobar G, Ranaudo MA, Khazen J, Borges B, Pereira JC, Méndez B (1999) *Energy Fuels* 13:333–335
8. Tomczyk NA, Winans RE, Shinn JH, Robinson RC (2001) *Energy Fuels* 15:1498–1504
9. Qian K, Robbins WK, Hughey CA, Cooper HJ, Rodgers RP, Marshall AG (2001) *Energy Fuels* 15:1505–1511
10. Robbins WK (1998) *Prepr Am Chem Soc Div Pet Chem* 43:137–140
11. Rudin J, Wasan DT (1992) *Colloids Surf* 68:67–79
12. Rudin J, Wasan DT (1992) *Colloids Surf* 68:81–94
13. Sjöblom J, Johnsen EE, Westvik A, Bergflødt L, Auflem IH, Havre TE, Kallevik H (2000) In: The 2nd international conference on petroleum and gas phase behaviour and fouling, Copenhagen, Denmark, 27–31 August 2000
14. Poggesi G, Hurtevent C, Buchart D (2002) In: SPE oilfield scale symposium, SPE74649 1-6, Aberdeen, UK, 2002
15. Gallup DL, Smith PC, Chipponeri J, Abuyazid A, Mulyono D (2002) In: SPE international conference on health, safety and environment in oil and gas exploration and production, SPE73960 1-16, Kuala Lumpur, Malaysia, 2002
16. Vindstad JE, Bye AS, Grande KV, Hustad BM, Hustvedt E, Nergård B (2003) In: 5th SPE oilfield scale symposium, SPE80375, Aberdeen, UK, 2003
17. Gossen PD, MacGregor JF, Pelton RH (1993) *Appl Spectrosc* 47:1852–1870
18. Pasikatan MC, Steele JL, Spillman CK, Haque E (2001) *J Near Infrared Spectrosc* 9:153–164
19. Frake P, Gill I, Luscombe CN, Rudd DR, Waterhouse J, Jayasorriya UA / (1998) *Analyst* 123:2043–2046
20. Santos AF, Lima EL, Pinto JC (1998) *J Appl Polym Sci* 70:1737–1745
21. Auflem IH, Havre TE, Sjöblom J (2002) *Colloid Polym Sci* 280:695–700
22. Aske N, Kallevik H, Johnsen EE, Sjöblom J (2002) *Energy Fuels* 16:1287–1295
23. Mullin JW (2001) *Crystallization*, 4th edn. Butterworth-Heinemann, Oxford
24. Wu W, Nancollas GH (1998) *Pure Appl Chem* 70:1867–1872
25. Chivate MR, Vaidya AM, Tavare NS (1976) *Indian J Technol* 14:569–572
26. Mullins OC (1990) *Anal Chem* 62:508–514
27. Kerker M (1969) In: Loebel EM (ed) *The scattering of light and other electromagnetic radiation*. Physical chemistry. A series of monographs, vol 16. Academic, New York, p 666
28. Heller W (1965) *J Chem Phys* 42:1609–1615
29. Mediaas H, Ardø BA, Grande K, Hustad BM, Rasch A, Rueslåtten H, Vindstad JE (2003) In: 5th SPE oilfield scale symposium, SPE80404, Aberdeen, UK, 2003
30. Aske N, Kallevik H, Sjöblom J (2002) *Appl Spectrosc* (accepted)
31. Mullin JW, Zacek S (1981) *J Cryst Growth* 53:515–518
32. Andreassen J-P (2001) *Growth and aggregation phenomena in precipitation of calcium carbonate*. Doctoral thesis, Department of Chemical Engineering, Norwegian University of Science and Technology, Trondheim
33. Matijevic E, Leja J, Nemeth R (1966) *J Colloid Interface Sci* 22:419–429
34. Young SL, Matijevic E (1977) *J Colloid Interface Sci* 61:287–301
35. Havre TE, Sjöblom J *Colloids Surf A* DOI 10.1016/s0927-7757(03)00302-9
36. Beneventi D, Carré B, Gandini A (2001) *J Colloid Interface Sci* 237:142–144
37. Mullin JW, Raven KD (1962) *Nature* 195:35–38
38. Mullin JW, Raven KD (1961) *Nature* 190:251